Int. J. Electrochem. Sci., 12 **(2017)** 4724 – 4732, doi: 10.20964/2017.06.58

International Journal of
ELECTROCHEMICAL
SCIENCE
www.electrochemsci.org

Facile Synthesis of Triply Hierarchical $NiCo_2O_4$ Arrays Grown on Ni Foam for electrode material of Supercapacitor

Tao Han[1], *Chongxu Wang*[2], *JunRui Yao*[2] , *Jianli Jin*[2], *Youyi Sun*[2,*], *Yinghe Zhang*[3], *Yaqing Liu*[2]

[1] School of Materials science and techology, North University of China, Taiyuan 030051, P.R.China.
[2] Shanxi Province Key Laboratory of Functional Nanocomposites, North University of China,Taiyuan 030051, China.
[3] Department of Nanotechnology, Helmholtz Association of German Research Centres, Hamburg 21502, Germany.
[*]E-mail: syyi@pku.edu.cn

Received: 13 February 2017 / *Accepted:* 23 April 2017 / *Published:* 12 May 2017

The triply hierarchical $NiCo_2O_4$ array grown on Ni foam ($NiCo_2O_4$/NF) was prepared by a facile hydrothermal method. Furthermore, the triply hierarchical $NiCo_2O_4$/NF exhibited higher specific capacitance (ca.2370.0F g^{-1}) comparing to the other $NiCo_2O_4$/NFs reported in previous works. At the same time, the capacitance loss was only 17.6% after 1000 charge-discharge cycling tests. The excellent specific capacitance and long cycle ability was attributed to the triply hierarchical structure. These results did not only synthesize triply hierarchical $NiCo_2O_4$/NF for application in electrode material of supercapacitors, but also proved that triply hierarchical arrays showed high capacitive properties.

Keywords: hydrothermal approach, Ni foam, mesoporous $NiCo_2O_4$ array, supercapacitor.

1. INTRODUCTION

Recently, spinel nickel cobaltite ($NiCo_2O_4$) as electrode material of supercapacitor has attracted lots of interesing due to be high theoretical capacitance, low cost and environmental friendliness[1-2]. It was well known that the $NiCo_2O_4$ arrays showed higher electrochemical performance comparing to the $NiCo_2O_4$ powder[3-5]. Hence, in the past years, the preparation and properties of $NiCo_2O_4$ arrays have been investigated for application in supercapacitor in detail[5-11]. For example, the dual hierarchical $NiCo_2O_4$ nanoneedle arrays grown on Ni foam was prepared by the hydrothermal method. The superior specific capacitance of 2193.0F/g was observed [5]. The dual hierarchical $NiCo_2O_4$ nanosheets arrays grown on Ni foam was also prepared by the two-step hydrothermal method. The

specific capacitance of 2623.3F/g was obtained at a current density of 1.0A/g[6]. The preparation and properties of dual hierarchical $NiCo_2O_4$ nanograss arrays grown on Ni foam was investigated in detail. It showed high capacitance of 2.1F/cm^2 at a current density of 2.0mA/cm^2 [7]. Zheng et al reported the synthesis of dual hierarchical $NiCo_2O_4$ nanowall arrays grown on Ni foam by one-step hydrothermal method. The high capacity (ca.130mAh/g) was achieved at 2.0A/g[8]. Xiong et al reported a two-step method for preparing ultrathin $NiCo_2O_4$ nanosheet arrays grown on Ni foam as a electrode materials of supercapacitor. It showed excellent specific capacitance of 1450.0F/g at 20.0A/g[9]. Despite the dual hierarchical $NiCo_2O_4$ arrays have been reported for application in electrode material of supercapacitor in these previous works. However, the preparation and properties of triply hierarchical $NiCo_2O_4$ arrays was few reported.

Herein, a triply hierarchical $NiCo_2O_4$ arrays grown on Ni foam was designed and prepared by a facile hydrothermal method. Furthermore, the electrochemical performance of triply hierarchical $NiCo_2O_4$ arrays was investigated in detail. Comparing to the dual hierarchical $NiCo_2O_4$ arrays reported in previous works, it showed higher electrochemical performance. These results provided a help for improving the performace of supercapacitor based on electrode material with multiple hierarchical structures.

2. EXPERIMENT

2.1 Preparation of $NiCo_2O_4$ arrays grown on Ni foam

The $NiCo_2O_4$/NF was synthesized by the one-step hydrothermal method as shown in following. The 0.29g nickeldinitrate hexahydrate, 0.58g cobaltousnitrate hexahydrate and 1.45g urea were dissolved in the 60ml mixing solution ($V_{water}/V_{ethanol}$=1:1). Afterwards, the NH_4F was added to the above mixing solution, which was further transferred to an Teflon-lined stainless-steel autoclave. And then, the Ni foam was also put in the Teflon-lined stainless-steel autoclave. In order to obtain triply hierarchical $NiCo_2O_4$ precursor, the reaction temperature was set at 105.0℃ for 6.0h. At last, the Ni foam containing red product was calcined at 300.0℃ in air for 2.0h. The active mass of $NiCo_2O_4$ measured by weight difference before and after the reaction.

2.2 Structure characterization

The crystalline structure of the product was determined by a Bruker D8 Avance X-ray diffractometer using Cu Ka radiation.

The morphology of the product was characterized by a field emission transmission electron microscope (TEM, JEOL 2100).

The morphology and element composition of the product was characterized by a field emission scanning electron microscope (FESEM, Hitachi S-4800) containing a Horiba EX-250 X-ray energy-dispersive spectrometer (EDS).

2.3 Electrochemical measurements

The electrochemical properties of $NiCo_2O_4$/NF electrode (1.0cm×2.0cm) were measured by three-electrode cell in 6 M KOH aqueous solution. The cyclic voltammetry (CV) and electrochemical impedance spectroscopy (EIS) were determined by the electrochemical workstation (CHI110, Austin, TX). The galvanostatic charge-discharge (GCD) was tested by the Wuhan LAND electronics (Land CT-2001A). The specific capacitance (*C*, F/g) was calculated according to the equation $C=I\times\Delta t/(m\times\Delta V)$. Where the m was the mass of the electroactive materials in the electrodes (g) , the I was the constant discharge current (A), the ΔV was potential drop during discharg (V) and the Δt was the total discharge time (s).

3. RESULTS AND DISCUSSION

The formation of $NiCo_2O_4$/NF was firstly confirmed by the XRD spectrum as shown in Fig.1A. Three sharp peaks of 44.4°, 51.8° and 76.3° were clearly observed, which were assigned to the (111), (200) and (220) planes of Ni, respectively (JCPDS card No. 04-0850)[12]. At the same time, some small diffraction peaks at 18.9°, 30.8°, 36.8°, 38.4° and 59.0° were also observed, which were assigned to (111), (220), (311), (222), and (511) planes of $NiCo_2O_4$, respectively(JCPDS card No. 73-1702)[13]. The EDS spectrum of the product was also characterized as shown in Fig.1B. There clearly showed the pattern peaks of Co, Ni and O, indicating that these elements (eg. Co, Ni and O) were existence in the products. Furthermore, the molar ratio of Ni: Co: O was about 1.0:1.9:4.0, which was consistent with the formula of $NiCo_2O_4$ [14]. These results indicated that the $NiCo_2O_4$/NF could be prepared by the one-step hydrothermal method.

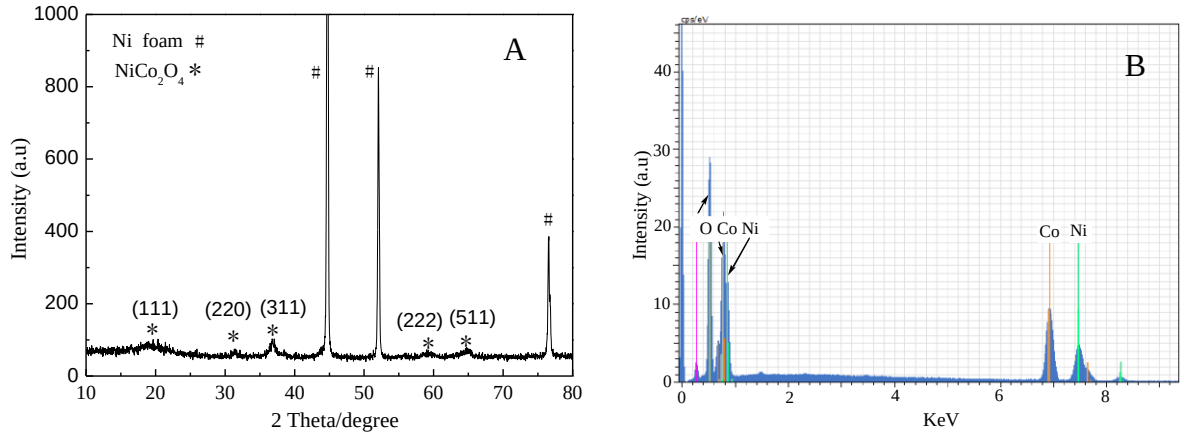

Figure 1. (A) XRD and (B) EDS spectrum of $NiCo_2O_4$/NF.

The triply hierarchical structure of $NiCo_2O_4$ arrays grown on Ni foam was firstly determined by the SEM images as shown in the Fig.2A-D. The microsheet array coated on the backbones of the Ni foam was clearly observed in the Fig.2A-B. As seen from Fig.2C-D, the microsheet was composed of mesoporous $NiCo_2O_4$ nanowires, in which the mesoporous $NiCo_2O_4$ nanowire resulted from the self-

assemble of $NiCo_2O_4$ nanoparticles. Fig.2E shows the TEM image of $NiCo_2O_4$ nanowire. It clearly showed that the nanowire with diameter of 45.0nm was self-assemble from nanoparticles with an average diameter of 6.0nm, forming mesoporous structure. Fig.2F shows the HRTEM image of $NiCo_2O_4$ nanowire. The lattice spacing was about 0.25nm, which was assigned to the (311) plane of $NiCo_2O_4$[15]. The electron diffraction (SAED) pattern of the $NiCo_2O_4$ nanowire was also characterized as shown in the inset of Fig.2E. It clearly showed the mesoporous $NiCo_2O_4$ nanowires to be polycrystalline. These results further confirmed the formation of triply hierarchical $NiCo_2O_4$ arrays.

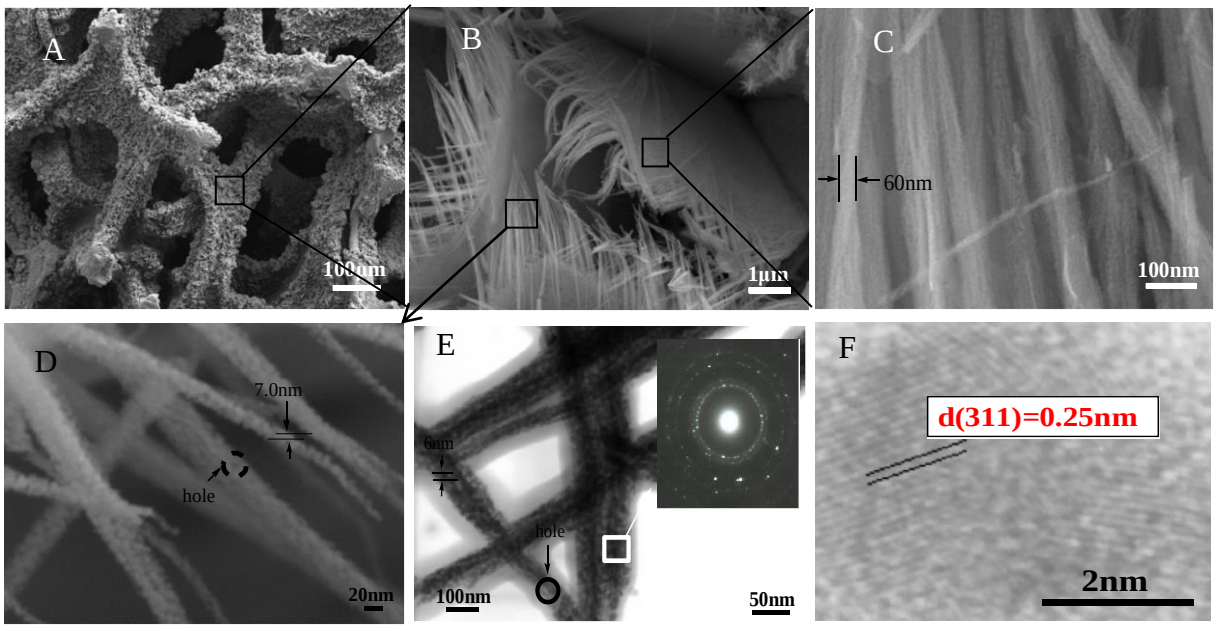

Figure 2. (A-D) SEM images of the $NiCo_2O_4$ arrays, (E) TEM image and (F) HRTEM image of the $NiCo_2O_4$ nanowires. The inset of E was the SAED pattern of $NiCo_2O_4$ nanowires.

Fig.3A shows the N_2 adsorption-desorption isotherms of the triply hierarchical $NiCo_2O_4$ arrays grown on Ni foam. The curve exhibited type IV isotherms, indicating the mesoporous structure of the $NiCo_2O_4$ arrays[6]. The BET surface area of the triply hierarchical $NiCo_2O_4$/NF was calculated to be about 62.4m^2/g. The $NiCo_2O_4$/NF showed a lower active surface comparing to $NiCo_2O_4$ reported in previous work as shown in Table 1. The result was due to Ni foam with low active surface. Only considering the weight of $NiCo_2O_4$ grown on Ni foam, the active surface was ca.3744.2m^2/g in present work, which was approximately 20 times higher than that in previous works [6, 10]. The pore size distribution was shown in Fig.3B, which came from the BJH method using the desorption branch of the nitrogen isotherm. The pore volume (0.26cm^3/g) of triply hierarchical $NiCo_2O_4$/NF was significantly high. The $NiCo_2O_4$/NF showed a wide pore size distribution of 5.0~15.0nm. The result was attributed to the triply hierarchical structures of 2D microsheet composed of 1D nanowire, resulting from self-assemble of spherical nanoparticles. These results indicated that the triply hierarchical structures showed a relatively higher specific surface area. Furthermore, the appealing textural properties may not only ensure a high electroactive surface area for redox reactions, but also permit easy ion access of the electrode/electrolyte interface as shown in Fig.3C.

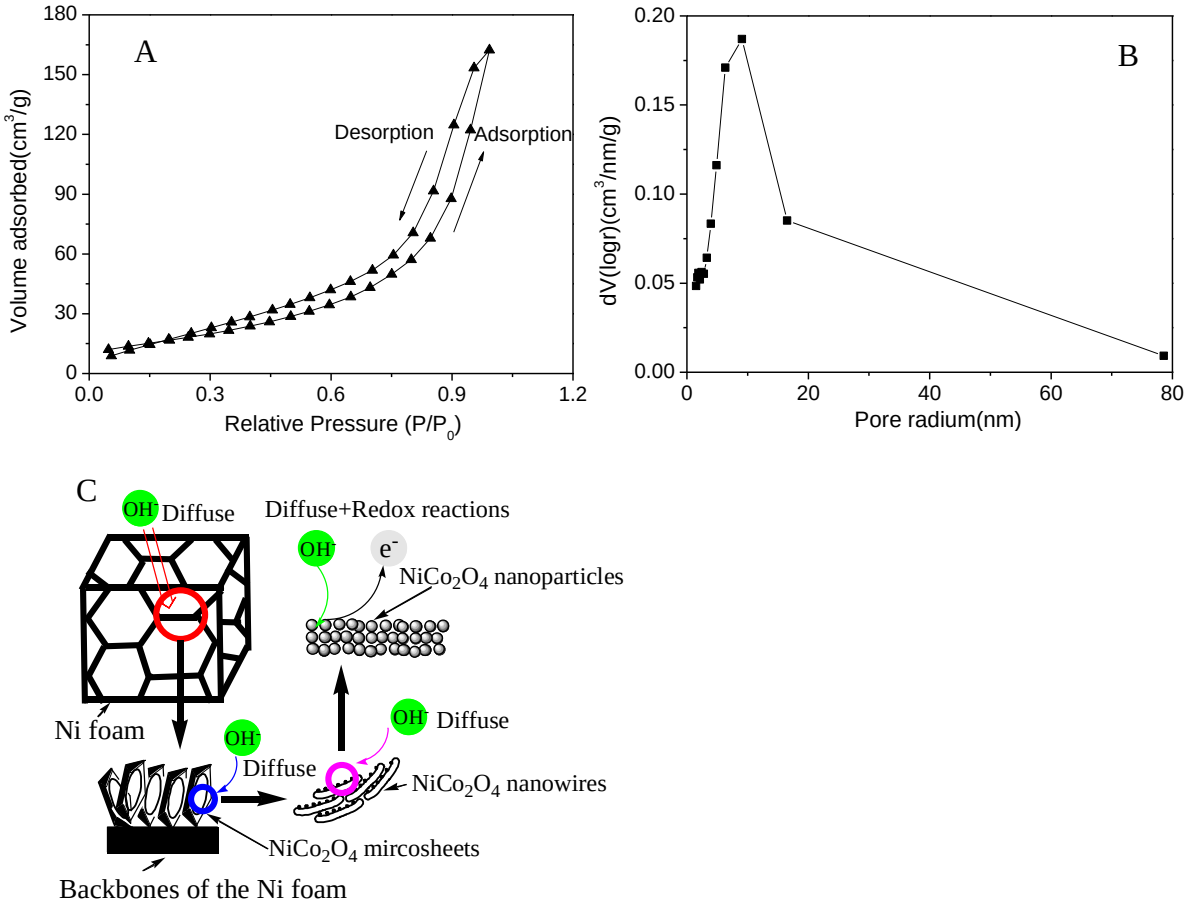

Figure 3. (A) Nitrogen adsorption−desorption isotherms and (B) pore size distribution curves of the $NiCo_2O_4$/NF . (C) is the schematic diagram of the triply hierarchical $NiCo_2O_4$ array grown on Ni foam.

The CV curves of the $NiCo_2O_4$/NF were characterized at various scan rates as shown in Fig.4. A couple of redox peaks of 0.18V~0.22V and 0.35V~0.42V were clearly observed for the $NiCo_2O_4$/NF electrode. The result indicated the faradaic capacitive behavior of $NiCo_2O_4$/NF electrode, in which the reaction of Co^{3+}/Co^{4+} and Ni^{2+}/Ni^{3+} transitions associated with anions OH^- was reversible[16]. In addition to this, all CV curves showed a similar shape. At the scan rate of 10.0mV/s, a pair of redox peaks of 0.21V and 0.33V were observed. When the scan rate was improved from 10.0mV/s to 100.0mV/s, the anodic and cathodic peak were blue and red shift to be 0.14V and 0.39V, respectively. It was interesting that the CV curve still clearly showed a pair of redox peaks at a high scan rate of 100.0mV/s. The result indicated the triply hierarchical $NiCo_2O_4$ arrays to be fast charge-discharge, which was attributed to the high interface area, easy ion diffusion and low resistance. Furthermore, the peak was only shifted to be ca. 60.0mV for a 10.0 times increase in the scan rate, which indicated the triply hierarchical electrode to be low polarization [17].

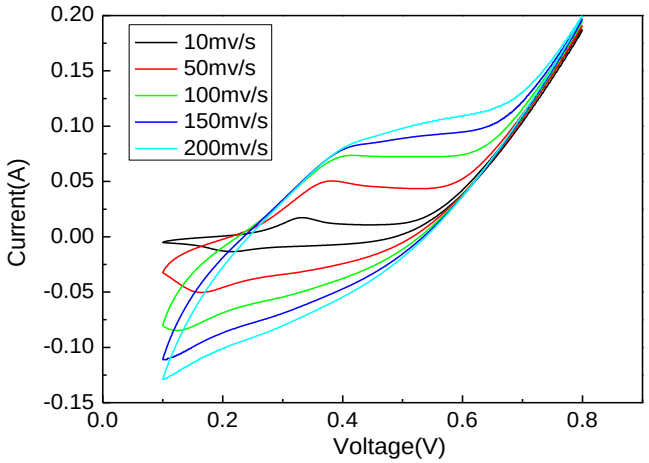

Figure 4. The CV curves of the $NiCo_2O_4$/NF at various scan rates.

The GCD curves of $NiCo_2O_4$/NF were determined at various current densities as shown in Fig.5A. The specific capacitance of $NiCo_2O_4$/NF was calculated to be 2370.0F/g,2062.0F/g, 2192.0F/g, 1942.0F/g and 2044.0F/g at the current density of 2.0A/g, 4.0A/g, 8.0A/g, 16.0A/g and 20.0A/g, respectively. At the same time, it showed that when the current was improved from 2.0A/g to 20.0A/g the specific capacitance of $NiCo_2O_4$/NF electrode still maintained its 86.2%. The cycling stability of $NiCo_2O_4$/NF electrode was further investigated at a current density of 2.0A/g for 1000 cycling tests as shown in Fig.5B. It clearly showed that the specific capacitance of $NiCo_2O_4$/NF electrode was still 1972.0F/g after 1000 cycling tests. The long cycle life of $NiCo_2O_4$/NF electrode was attributed to its triply hierarchical structure and good adhesion between $NiCo_2O_4$ microsheet arrays and Ni foam. The above results further demonstrated that the $NiCo_2O_4$ arrays with triply hierarchical structure exhibited high performance of supercapacitors.

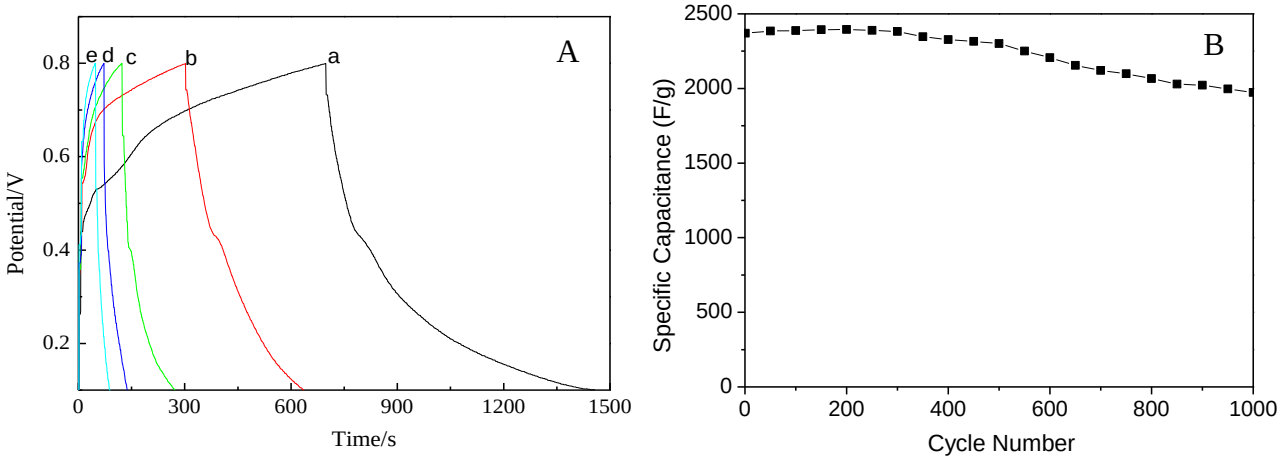

Figure 5. (A) The GCD curves of the $NiCo_2O_4$/NF at various current densities of (a) 2.0A/g, (b) 4.0A /g, (c) 8.0A/g,(d) 16.0A/g and (e) 20.0A/g, (B) is cycling performance of $NiCo_2O_4$/NF at a current density of 2.0A/g.

The specific capacitance of $NiCo_2O_4$/NF with various hierarchical structures was conclude and compared in Table 1. It was found that the $NiCo_2O_4$/NF with triply hierarchical structure had the highest value comparing to $NiCo_2O_4$/NF with dual or single hierarchical structure reported in previous

works. The excellent specific capacitance of $NiCo_2O_4$/NF in the present work could be ascribed to the unique triply hierarchical structure with several advantages. Firstly, the triply hierarchical $NiCo_2O_4$ arrays provided the larger active surface comparing to previous works[6,10]. Secondly, the $NiCo_2O_4$ nanowires with mesoporous structure reduced the diffusion distance of electrolytes into the surface of electrode materials. In addition, the triply hierarchical $NiCo_2O_4$ arrays provided more channels, which was benefited OH^- ions easy diffusion to the inner of electrode materials, accelerating the interfacial reaction as shown in Fig.3C. Finally, the triply hierarchical structure also enhanced adhesion between the Ni foam and the $NiCo_2O_4$ arrays, resulting in improvement of structure stability during galvanostatic charge-discharge process[18]. These characteristics made the triply hierarchical $NiCo_2O_4$ arrays grown on Ni foam to act as a kind of good electrode materials of electrochemistry energy storage.

Table 1. The comparison in properties of $NiCo_2O_4$/NF with various hierarchical structures.

Array Structures	Hierarchical Structures	Surface area(m^2/g)	Capacitance/F/g (current density)	Re.
Microsheet/nanowire /nanoparticle	triply	64.2	2370.0(2.0A/g)	present
Nanoneedle/nanoparticle	dual	------	2193.5(1.0A/g)	5
Nanosheet/nanowire	dual	------	1859.0(4.0A/g)	9
Nanograss/nanoparticle	dual	------	1136.1(5.0A/g)	7
Nanowire	single	104.8 (without Ni)	1481.0(2.0A/g)	6
Nanoneedle	single	------	1189.6(1.0A/g)	3

The EIS of triply hierarchical $NiCo_2O_4$/NF was further characterized as shown in Fig.6A. It clearly showed that the impedance plot of triply hierarchical $NiCo_2O_4$/NF electrode was straight line, indicating excellent capacitive behavior [18]. At the same time, the equivalent series resistance (ESR) of 0.56 Ω and charge-transfer resistance (Rct) of 0.46Ω were observed, indicating a low internal resistance and a short ion diffusion path for the triply hierarchical $NiCo_2O_4$/NF electrode[19-20]. Here, the result was due to the binder-free nature of the $NiCo_2O_4$/NF electrode and a good connection between the triply hierarchical mesoporous $NiCo_2O_4$ array and Ni foam. Furthermore, the EIS of $NiCo_2O_4$/NF electrode before and after 1000 cycling tests was also compared as shown in Fig.6A. The ESR of $NiCo_2O_4$/NF electrode was slight change after 1000 cycling tests. The result indicated that the internal resistance of the $NiCo_2O_4$/NF was slightly affected by the charge-discharge process. However, a slight increase in *R*ct of $NiCo_2O_4$/NF electrode was observed after 1000 cycling tests as shown in Fig.6A. The result indicated that the interface resistance for ion diffusion into electrode was improved after 1000 cycling tests. Fig.6B-C shows the SEM images of triply hierarchical $NiCo_2O_4$ arrays after 1000 cycles. The microsheet arrays kept well and was few destroyed, and the nanowires were completely destroyed. In addition to this, it was interesting that the mesoporous structure kept also well

due to the aggregates of $NiCo_2O_4$ nanoparticles. The result was key role for the long cycle ability of this triply hierarchical $NiCo_2O_4$ arrays.

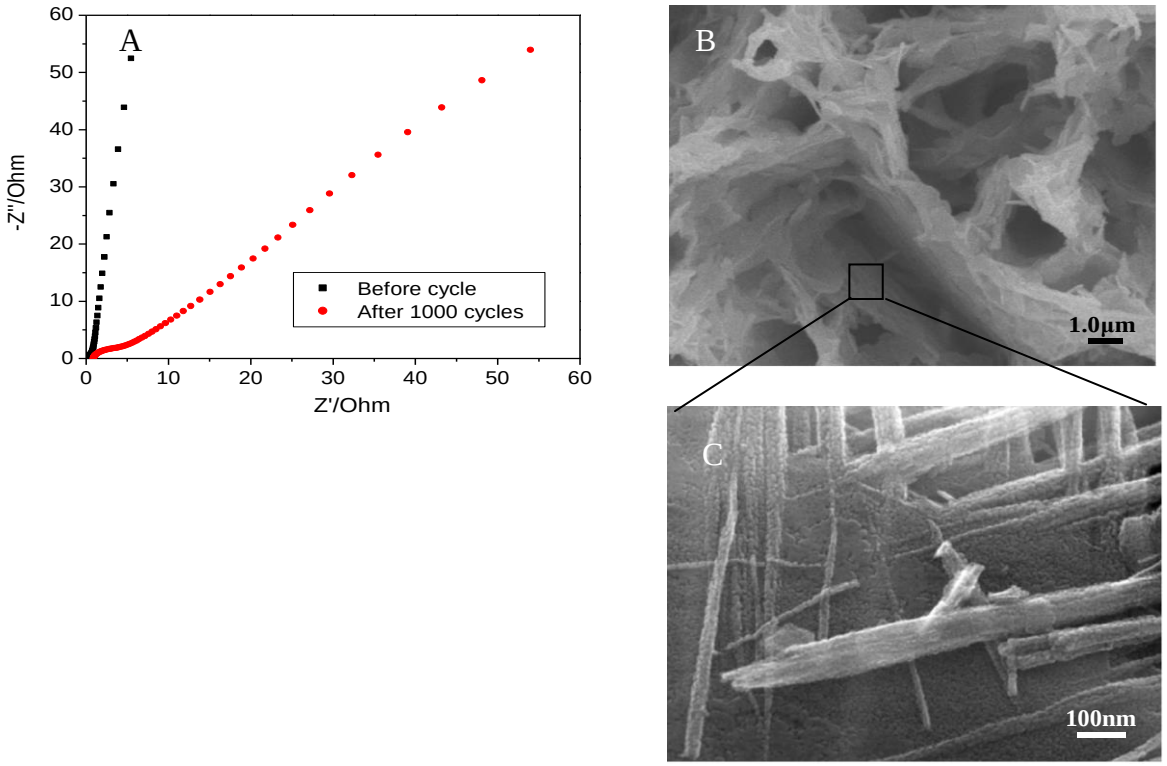

Figure 6. (A) Nyquist curve of the 1st and 1000th cycle of the $NiCo_2O_4$/NF electrode. (B-C) are the SEM images of 1000th cycle of the $NiCo_2O_4$/NF electrode.

4. CONCLUSIONS

In summary, triply hierarchical $NiCo_2O_4$ arrays grown on Ni foam have been successfully prepared by a facile hydrothermal method. Our results demonstrated that the triply hierarchical $NiCo_2O_4$ array electrode exhibited higher capacitance and better cycling stability comparing to $NiCo_2O_4$ array with dual and single hierarchical structures. This result was attributed to that the triply hierarchical structures were advantageous for efficient ion and electron transport and could better accommodate the volume changes. Other electrode materials with triply hierarchical structures were explored to further improve performance of supercapacitor in the future.

ACKNOWLEDGEMENTS
The authors are grateful for the support by National Natural Science Foundation of China under grants (11202006), the Shanxi provincial natural science foundation of China (2014011003-2) and Special Foundation for State Major Basic Research Program of Shanxi (MC2016-02).

References

1. J. F. Shen, X. F. Li, N. Li and M. X. Ye, *Electrochim. Acta.*, 141 (2014) 126.
2. 2. V. H. Nguyen and J. J. Shim, *J. Power Sources.*, 273 (2015) 110.

3. G. Q. Zhang, H. B. Wu, H. E. Hoster, M. B. Chan Park and X. W. (David) Lou, *Energy Environ. Sci.*, 5 (2012) 9453.
4. 4. Q. F. Wang, X. F. Wang, B. Liu, G. Yu, X. J. Hou, D. Chen and G. Z. Shen, *J. Mater. Chem A.*, 1 (2013) 2468.
5. 5. J. Wu, R. Mi, S. M. Li, P. Guo, J. Mei, H. Liu, W. M. Laua and L. M. Liu, *RSC Adv.*, 5 (2015) 25304.
6. 6. Q. W. Zhou, J. C. Xing, Y. F. Gao, X. J. Lv, Y. M. He, Z. H. Guo and Y. M. Li, *ACS Appl. Mater. Interfaces.*, 6 (2014) 11394.
7. Z. Y. Wang, Y. F. Zhang, Y. H. Li and H. Y. Fu, *RSC Adv*., 4 (2014) 20234.
8. 8. Q. Y. Zheng, X. Y. Zhang and Y. M. Shen, *Mater. Res. Bull.*, 64 (2015) 401.
9. C. Z. Yuan, J. Y. Li, L. R. Hou, X. G. Zhang, L. F. Shen and X. W. (David) Lou, *Adv. Funct. Mater.*, 22 **(**2012) 4592.
10. T. Peng, Z. Y. Qian, J. Wang, L. T. Qu and P. Wang, *Phys. Chem. Chem. Phys.*, 17 (2015) 5606.
11. 11. J. B. Cheng, Y. Lu, K. W. Qiu, D. Y. Zhang, C. L. Wang, H. L. Yan, J. Y. Xu, Y. H. Zhang, X. M. Liu and Y. S. Luo, *Cryst. Eng. Comm.*, 16 (2014) 9735.
12. 12. Y. Y. Sun, W. H. Zhang, D. S. Li, L. Gao, C. L. Hou, Y. H. Zhang and Y. Q. Liu, *J. Alloys Compd.*, 649 (2015) 579.
13. X. Xiao, F. Yang, K. Cheng, X. Wang, J. L. Yin, K. Ye, G. L. Wang and D. X. Cao, *J. Electroanal. Chem.*, 729 (2014) 103.
14. Q. Zhang, Y. H. Deng, Z. H. Hu, Y. F. Liu, M. M. Yao and P. P. Liu, *Phys. Chem. Chem. Phys.*, 16 (2014) 23451.
15. H. Wang and X. Wang, *ACS Appl. Mater. Interfaces.*, 5 (2013) 6255.
16. H. Jiang, J. Ma and C. Li, *Chem. Commun.*, 48 (2012) 4465.
17. Y. Y. Sun, W. H. Zhang, D. S. Li, L. Gao, C. L. Hou, Y. H. Zhang and Y. Q. Liu, *Electrochim. Acta.*, 178 (2015) 823.
18. G. Q. Zhang and X. W. Lou, *Sci. Rep.*, 3 (2013) 1470.
19. C. Z. Yuan, L. Yang, L. R. Hou, L. F. Shen, X. G. Zhang and X. W. Lou, *Ener.Environ. Sci.*, 5 (2012) 7883.
20. 20. Y. Huang, Y. Y. Li, Z. Q. Hu, G. M. Wei, J. L. Guo and J. P. Liu, *J. Mater. Chem. A.*, 1 (2013) 9809.